MoonLIGHT

S. Dell'Agnello, L. Porcelli, M. Tibuzzi, L. Salvatori, M. Muccino, L. Filomena, M. Montanari, L. Rubino, L. Mauro, A. Remujo Castro, M. Petrassi, M. Traini, U. Denni

1 Introduction

Laser Ranging (LR) is a technique used to perform accurate precision distance measurements between a laser ground station and an optical target, a Cube Corner Retroreflector (CCR). Since 1969 it is possible to realize Lunar Laser Ranging (LLR) measurements thanks to the Apollo and Luna missions that placed some arrays of CCRs on the lunar surface. LLR outputs include accurate tests of theories of gravity, information on the composition of the Moon, its ephemerides, and its internal structure or geocentric positions, and motions of ground stations: research uniquely enabled by the Moon.
Despite laser ground stations having significantly improved over the years, the current limitation of the lunar optical target is due to lunar librations [1]. In order to achieve more precise LLR measurements, Moon Laser Instrumentation for General relativity High accuracy Test (MoonLIGHT) project is designed by SCF_Lab[1] in collaboration with the University of Maryland. The aim of the project is to design next-generation retroreflectors (prototyping and manufacturing) and qualify them for the Moon's environment. Thus, we move from a multi-small CCRs array to a single large 100 mm CCR, i.e. MoonLIGHT, unaffected by the lunar librations [2].
The field of view of each CCR is limited: the retroreflector needs to be pointed precisely to the ground station. The Apollo CCR arrays were manually arranged by the astronauts. In 2018 INFN proposed to ESA the MoonLIGHT Pointing Actuators (MPAc) project, able to perform unmanned pointing operations of MoonLIGHT. In 2019 ESA chose MPAc among 135 eligible scientific project proposals. In 2021 ESA agreed with NASA to launch MPAc to the Reiner Gamma region of the Moon, with Commercial Lunar Payload Services (CLPS), which is part of the Artemis program. The lander on which MPAc will be integrated is designed by Intuitive Machines (IM). The launch expected date is in April 2024 [3].

[1] Satellite/lunar/GNSS laser ranging/altimetry and Cube/microsat Characterization Facilities Laboratory.

2 Science objectives of MoonLIGHT

The request of understanding large-scale gravity has been one of the great spurs to the development of scientific inquiry throughout history. At every stage, there has unfolded the great interplay between measurement and model which is at the heart of the scientific process, as new measurements, often permitted by novel techniques, have challenged the paradigm of the day and ushered in some new understanding.
GR is currently the final paradigm to develop predictions over gravitational physics at large scales. But do we today have in hand a perfect theory of gravitation, with which no valid measurement will ever be found to disagree? It is not surprising that when Einstein first formulated GR, only the pristine gravitational laboratory of the solar system offered a venue in which its predictions could be compared with those of Newton. Of course, the new theory appeared to pass the tests of the time, of the precession of the perihelion of Mercury and the deflection of starlight by the sun, and so became a standard that would not face another experimental challenge for decades. In the last 50 years, a steady flow of increasingly precise solar-system measurements has greatly increased the rigor with which gravitation can be tested. More generally, technological advancements have enabled scientists to conduct increasingly in-depth studies of the cosmos over time. For instance, observations from Supernovae type Ia (SNe Ia), Cosmic Microwave Background radiation (CMB), Large Scale Structures (LSS), Baryon Acoustic Oscillations (BAO), and weak lensing provide information about the universe's dynamics as well as its kinematics. Indeed, they suggest that small perturbations occurred in the early universe and that the famous Friedmann Robertson Walker (FRW) metric perturbations formed cosmic structures. They also show an accelerated expanding universe with a flat spatial curvature. Consequently, also the theoretical landscape is very fertile: a diverse array of efforts aimed at producing a unified physical theory, that could explain all of these observations, have resulted in predictions that may be testably different from those of GR. In this context, the so-called "alternative theories of gravity", that is, all those theories that extend or modify the GR, arise too.
For years, SLR-LLR data have made it possible to test gravity in the weak-field slow-motion (WFSM) regime. Now our long-term goal is to study which of these new theories can be tested using data collected from upcoming LR missions. To achieve this ambitious goal, the first step is to determine the appropriate framework that will help to compare theoretical model with experimental data. The theoretical model must accurately reproduce observations, not just in the simplest way feasible. In fact, too many simplifications may result in a model that does not match reality. Once the theoretical background has been determined, we use experimental data from space missions to determine the value of the free parameters of the theory we would like to test.
The PPN formalism is the most suitable in the description of low gravity [4]. It is characterized by a set of eleven parameters whose values differ from one theory to another, see Tab.1.

Parameter	What it measures relative to GR
γ	How much space-curvature produced by unit rest mass?
β	How much "non - linearity"in the superposition law for gravity?
ξ	Preferred - location effects?
α_1	Preferred - frame effects?
α_2	
α_3	
α_3	Violation of conservation of total momentum?
ζ_1	
ζ_2	
ζ_3	
ζ_4	

Table 1: *Table on PPN parameters and their physical meaning [4].*

The value of the PPN parameters changes according to the theory under investigation. Consequently, experiments that measure PPN parameters can be used to test gravity theories: depending on the measured values, we can determine which theoretical model best fits the observations.
In this context, we analyzed some metric theories of gravity[2] (in addition to GR). The first one is the scalar-tensor theory, which has been introduced primarily as dark energy-free cosmological models and in the investigation of unification schemes such as strings. In its action[3]

$$\mathcal{A}_{\rm ST} = \frac{1}{16\pi}\int \left[\phi R - \phi^{-1}\omega(\phi) g^{\mu\nu}\phi_{,\mu}\phi_{,\nu} + 2\phi\lambda(\phi)\right]\sqrt{-g}d^4x + \mathcal{A}_{\rm m}, \qquad (1)$$

the metric $g_{\mu\nu}$ and the scalar field ϕ are two dynamic gravitational variables; there are also two arbitrary functions of the scalar field, the coupling function $\omega(\phi)$ and the cosmological one $\lambda(\phi)$.
Then, we studied Brans-Dicke's theory, which is a particular scalar-tensor theory with $\omega = \omega_{BD}$ constant and $\Lambda = 0$

$$\mathcal{A} = \frac{1}{16\pi}\int \left[\phi R - \phi^{-1}\omega_{BD} g^{\mu\nu}\phi_{,\mu}\phi_{,\nu}\right]\sqrt{-g}d^4x + \mathcal{A}_m. \qquad (2)$$

Finally, one of the most generic and simple extensions of GR: the $f(R)$ theory

$$\mathcal{A}_{f(R)} = \int d^4x\sqrt{-g}f(R) + \mathcal{A}_m, \qquad (3)$$

where $f(R)$ is a generic function of the curvature scalar R.
For each of these theories we collected the PPN parameters, listed in Tab.2.

[2]We refer to metric theories of gravity (such as GR) when matter and other non-gravitational fields are coupled only to the metric, and they satisfy the Equivalence Principle by construction.

[3]$\mathcal{A}_{\rm m}$ is the matter action, R is Ricci curvature tensor.

Theory	PPN parameters					
	γ	β	ξ	α_1	α_2	(α_3, ζ_i)
General Relativity	1	1	0	0	0	0
Scalar-tensor	$1+\Lambda$	0	0	0	0	0
Brans-Dicke	1	0	0	0	0	0
$f(R)$	$1-\frac{f''(R)^2}{f'(R)+2f''(R)^2}$	$1+\frac{1}{4}\frac{f'(R)f''(R)}{2f'(R)+3f''(R)^2}\frac{d\gamma}{dR}$	0	0	0	0

Table 2: *PPN parameters in metric theories of gravity: GR, scalar-tensor, Brans-Dicke [4], and $f(R)$ [5]. In the latter case, the prime indicates the derivative of $f(R)$ w.r.t. R.*

After defining the theoretical framework, one can proceed to the analysis of physical phenomena. One of the effects extensively investigated in the Solar System via the LR technique is the frame dragging. When Einstein began formulating his theory of GR, he attempted to incorporate Mach's principle, which states that rotations and accelerations relative to fixed and distant masses in the universe ("distant stars") cause the appearance of inertial forces. For instance, a clock that co-rotates at a constant distance around a spinning body will result forward in the starting point relative to a second clock at rest there; contrariwise, a counter-rotating clock will be behind the other one in that same point [6]. Thus, a particle orbiting a rotating body undergoes precession. The first frame dragging effect was derived in 1918 by the Austrian physicists Josef Lense and Hans Thirring, and it is also known as the Lense-Thirring effect

$$\frac{d\mathbf{S}}{d\tau} = \mathbf{\Omega_{LT}} \times \mathbf{S}, \quad \mathbf{\Omega}_{\rm LT} = -\frac{1}{2}\nabla \times \mathbf{g} = \frac{1}{2}\left(\frac{\alpha_1}{4}+\gamma+1\right)\frac{3(\mathbf{J}\cdot\hat{\mathbf{r}})\hat{\mathbf{r}}-\mathbf{J}}{r^3}. \qquad (4)$$

Here, $\mathbf{S}$ is the spin of a gyroscope orbiting a rotating body, $\mathbf{\Omega}_{\rm LT}$ is the rate of precession, and $\mathbf{J}$ is the angular momentum of the rotating body.
Numerous experiments conducted in the Solar System aim to quantify this effect, even though it is minimal in the weak field. Today, the goal of new space missions is to improve the accuracy of previous missions' measurements as well as to test the precession also in alternative theories of gravity. For this reason, we calculated the Lense-Thirring precession in the alternative theories of gravity seen before, as reported in Tab.3. The next step will be to constrain the free parameters of these theories using experimental measurements of the Lense-Thirring effect obtained from the LLR.

Theory	$\boldsymbol{\Omega}_{\rm LT}$
General Relativity	$\frac{3(\mathbf{J}\cdot\hat{\mathbf{r}})\hat{\mathbf{r}}-\mathbf{J}}{r^3}$
Scalar-tensor	$\left(\frac{3+2\omega}{4+2\omega}\right)\frac{3(\mathbf{J}\cdot\hat{\mathbf{r}})\hat{\mathbf{r}}-\mathbf{J}}{r^3}$
Brans-Dicke	$\left(\frac{3+2\omega_{BD}}{4+2\omega_{BD}}\right)\frac{3(\mathbf{J}\cdot\hat{\mathbf{r}})\hat{\mathbf{r}}-\mathbf{J}}{r^3}$
$f(R)$	$\left[\frac{2f'(R)+5f''(R)^2}{2f'(R)+4f''(R)^2}\right]\frac{3(\mathbf{J}\cdot\hat{\mathbf{r}})\hat{\mathbf{r}}-\mathbf{J}}{r^3}$

Table 3: *The Lense-Thirring effect in metric theories of gravity. For more details, see [7].*

3 MoonLIGHT

The current lunar payloads, i.e. Apollo 11, Apollo 14, Apollo 15, Lunokhod 1 and Lunokhod 2, are arrays composed by small CCRs with a diameter of 3.8 cm. Their design produces strong limitations in LLR measurements due to a lunar phenomenon, called lunar librations. The librations derive from the eccentricity of the Moon's orbit around the Earth: during the 28 days lunar phase, the Moon's rotation alternatively leads and lags its orbital position, of about 8 degrees. Therefore, the arrays are moved and one corner of the array is more distant than the opposite by several centimeters. For this reason, the dimension of the pulse coming back to the Earth is greater proportionally to the array physical dimensions and to the Moon-Earth distance increase (in the position in which the libration phenomena are at the peak).
In order to reduce the uncertainty of the LLR measurements, the ground stations like APOLLO use the photon number: it is possible to reach the millimiter level reducing the uncertainty of $\sqrt{N}$, i.e. through a greater photon rate [8]. Therefore without hardware upgrades of lunar retroreflectors, the only available improvement is on the timing of an extremely large number of photoelectron returns to reduce the errors by the root mean square of the single photoelectron measurement. The SCF team, in collaboration with the University of Maryland, proposed the 2$^{\rm nd}$ generation of lunar CCR, with a new design unaffected by lunar librations [9]. The key idea is to use, instead of an array of multiple small CCRs (for example 3.8 cm of front face diameter for Apollo), a series of single big retroreflectors, each one with 10 cm of front face diameter, called MoonLIGHT, deployed separately on the lunar surface. This new design creates single short reflected pulses with a final precision expected to be better than a few millimeters. Once this new kind of CCR will be deployed on the Moon, further improvements in the laser ground stations capabilities with shorter laser

pulses will be more effective.
Thus, it is possible to compare the evolution of the LLR in terms of measurements uncertainty: in the past the laser pulse was wide, bigger than the array dimensions; for this reason, the uncertainty is dominated by the laser. Now the laser pulse is improved, but there are still large arrays; therefore the uncertainty is dominated by the arrays. In the future, with MoonLIGHT, there will be a single large CCR minimizing the effect of librations. The uncertainty will be dominated by the laser pulse again; but the modern technology can do shorter laser pulses.

4 MPac

MPAc was designed for the alignment of a retroreflector in Azimuth and Elevation with respect to the Earth in the lunar environment [10]. Unlike the Apollo CCR arrays, that were manually arranged by the astronauts, MPAc has been developed for the lunar environment to perform unmanned pointing operation of MoonLIGHT.
MPAc is a double pointing actuator, equipped with MoonLIGHT 100 (ML100). ML100 is a CCR, with 100 mm of front face diameter. In order to point MoonLIGHT to the Earth direction, MPAc must be able to perform two continuos rotations. The current design is shown in Fig.1. In order to better analyze the

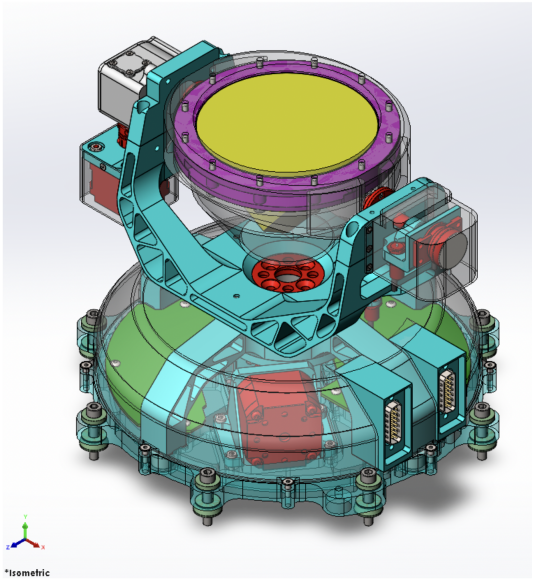

Figure 1: Current design of MPAc.

MPAc design, it is possible to divide ideally the entire structure into three parts.

1. **Azimuth block**: the lower part of MPAc represents the interface with the lander and it is fixed with respect to it. This block contains most of the electronics and the motor responsible of generating the Azimuth movement. The Azimuth rotation is around the normal to the (horizontal) lander deck surface with an ideal range of $\pm 180°$; for safety reasons, the real range of movements is limited by two Limit Switches. It holds the rest of the structure.

2. **Elevation block**: this block generates the Elevation rotation around an axis parallel to the lander deck. Its ideal range is $\pm 90°$; as in the Azimuth block, for safety reasons, the real range of movements is limited by two Limit Switches. The Elevation block contains the motor responsible of generating the Elevation movement and is responsible of holding the last block, the CCR Housing.

3. **CCR Housing**: the last block contains ML100 retroreflector, with its integration structure. It is a completely passive block; its function is to hold and protect the CCR.

With new CCRs on the Moon, we look forward to further improvements in range uncertainty and the resulting science.

5 Optical simulations

A perfect corner cube retroreflector reverses the direction of an incoming laser beam, but the reflected beam has a diffraction pattern [11].
Since the laser source is moving with respect to the CCR, as seen from the Moon the apparent positions of the Earth station at the transmit and receive times will be different. This aberration, due to velocity v, is $2v/c$ in radians or 412530 v/c in seconds of arc, where c is the speed of light. Velocity v is the component perpendicular to the line of sight. The orbital speed of the Moon is about 1.0 km/s and the equatorial rotational velocity of the Earth is 465 m/s. The equator plane of the Earth is tilted by 23.44° to the ecliptic plane whereas the lunar equator is tilted by 1.54° to the ecliptic plane. There is variety in the orientations of the Earth and Moon with respect to one another and with respect to the ecliptic plane. In addition, the lunar orbit is not circular so its orbital speed varies ± 0.1 km/s. Considering these complexities, the size of the aberration varies. For station latitudes of 30° to 50°, the most probable Velocity Aberration (VA) is between 1.0" and 1.1" (or, equivalently, between 4.84 μrad and 5.33 μrad) in longitude.
We must therefore take all of this into account when performing the optical simulations of the CCRs, which are crucial for understanding the return of light observed when the laser comes back to the station.
Code V is a software developed by Synopsys to model, optimize, and investigate optical systems for several applications.
At the SCF_Lab, Code V is utilized to simulate the optical performances of

single (or arrays of) CCRs employed in space missions [7, 11]. These simulations are compared with the optical experimental data obtained from tests on the actual payloads [12]. Code V features a graphical user interface that enables command entry and simulation execution. The software is also user-friendly because it supports the use of macros written in Macro PLUS programming language. These macros can be written on a text editor and then interpreted by the software. To initialize the simulation of the specific CCR under examination, some key parameters are required

- the diameter (or aperture) D;
- the Dihedral Angle Offsets (DAOs);
- the type of polarization;
- the laser beam wavelength λ;
- the incidence angle of the laser beam on the CCR front face;
- the material;
- the reflectivity ρ.

Additionally, the grid's dimensions and spacing are appropriately entered to produce an image with the desired resolution and size. Each run produces three plots

1. the average laser return's Far Field Diffraction Pattern (FFDP);
2. the laser return as a function of VA averaged over the azimuth angle;
3. the laser return of the total pattern as a function of the azimuth angle for a fixed VA.

In all of these plots, the laser return strength is quantified in absolute Optical Cross Section (OCS) units, i.e. in Msqm (million square meters, Msqm). These units derive from Degnan's equation describing the central peak of the laser return signal for a CCR with zero DAOs [13]. In his formula

$$\mathrm{OCS} = p\left(\frac{\rho\pi^3 D^4}{4\lambda^2}\right) = (168 - 670)\,\mathrm{Msqm} \tag{5}$$

for normal incidence of the laser beam on the CCR front face. The lower limit on the peak of the OCS is attained for $\lambda = 1064$ nm, whereas the upper limit is for $\lambda = 532$ nm. The factor $p = 26.4\%$ describes the effect of the polarization and applies only in the case of uncoated CCRs [14]. Non-zero DAOs reduce the value of the peak of the OCS in a nonlinear way.
The results of the simulations of a MoonLIGHT CCR with the following characteristics

- diameter D = 100 mm;

- DAOs = $(0, 0, 0)$";
- horizontal linear polarization;
- two laser beam wavelengths of $\lambda = 532$ nm and $\lambda = 1064$ nm;
- normal incidence of the laser beam on the CCR front face;
- uncoated Suprasil 311 fused silica CCR (index of refraction n = 1.456 − 1.463);
- reflectivity $\rho = 0.93$.

are shown in Figs.2-3. The FFDP of an uncoated 100 mm CCR with null DAOs shows a central lobe with six lateral ones of lower intensity. The peak intensity turns out to be at 669 Msqm when $\lambda = 532$ nm and at 165 Msqm when $\lambda = 1064$ nm, in agreement with the theoretical expected values predicted by Eq.(5). We conclude that zero DAOs are optimum for green and IR laser beams.

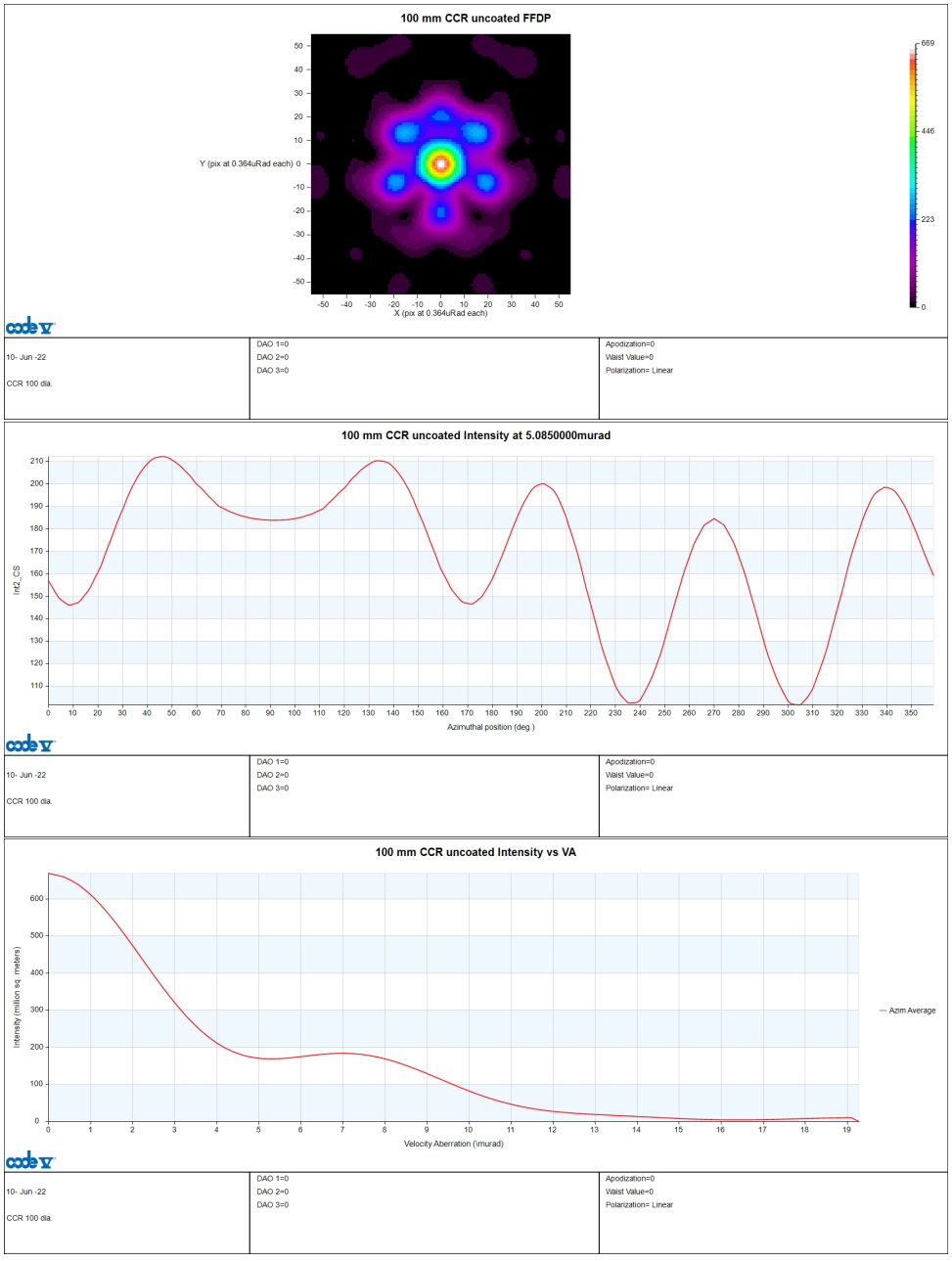

Figure 2: $\lambda = 532$ nm, linear polarization, and DAOs $= (0, 0, 0)''$: top, FFDP; middle, OCS vs. VA; bottom, OCS at VA 1.05" vs. azimuth angle.

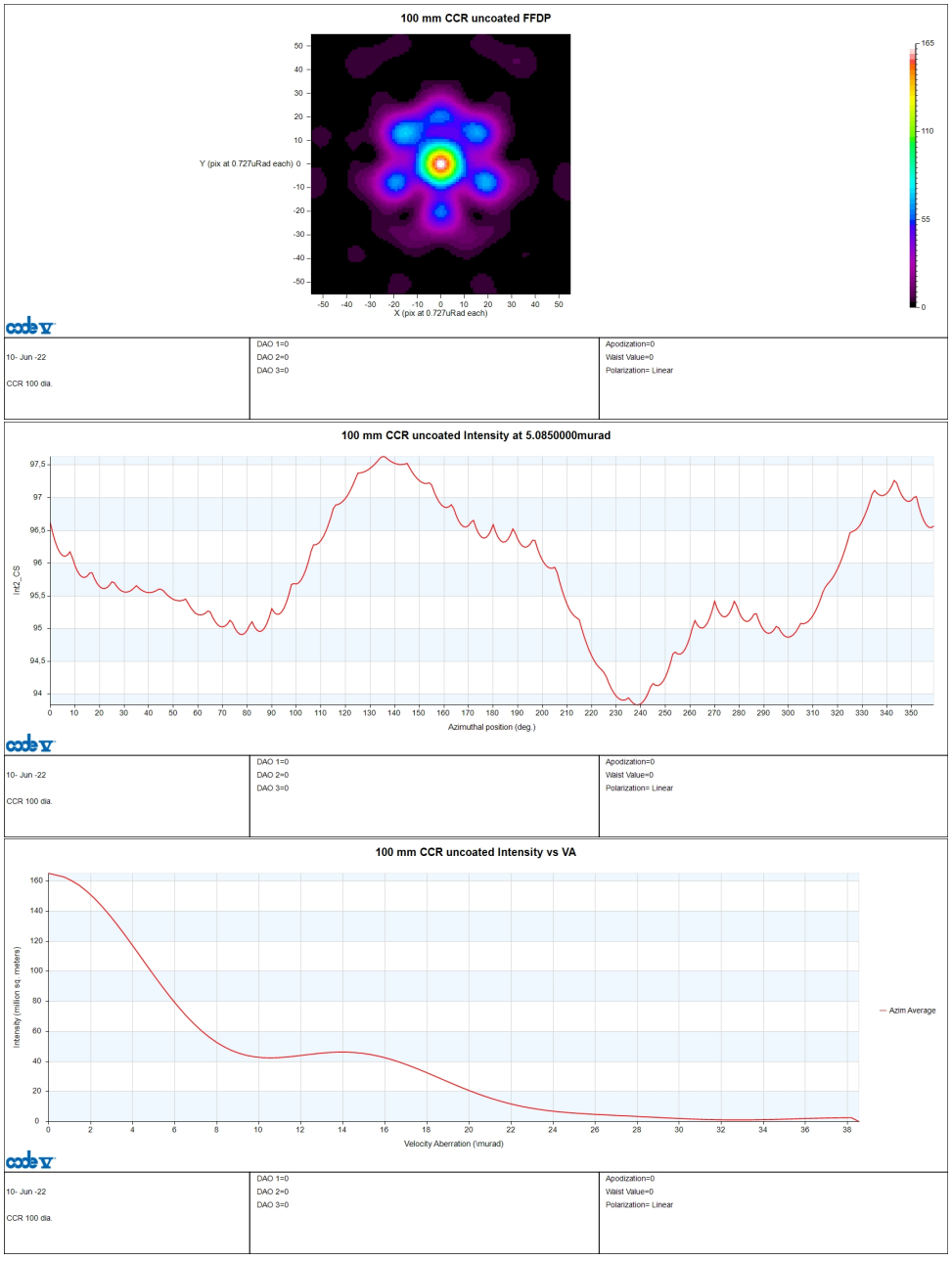

Figure 3: $\lambda = 1064$ nm, linear polarization, and DAOs $= (0, 0, 0)$": top, FFDP; middle, OCS vs. VA; bottom, OCS at VA 1.05" vs. azimuth angle.

6 Planetary Ephemeris Program

Planetary Ephemeris Program (PEP) represents a powerful software written in FORTRAN developed at CfA by I. Shapiro and collaborators during the fall of the 1960s. The program was initially thought to produce ephemeris data, but it was soon clear that other applications would mainly be implemented in the software. To this end, the program compares GR predictions with modern observations besides generating ephemerides of planets and the Moon. As a consequence, PEP has been and is still used to investigate departures from GR's predictions by placing limits over the PPN parameters β and γ, the geodetic precession and the variation of the gravitational constant G [15, 16, 17], and to measure the lunar geodetic precession [18]. PEP handles diverse sets of observations, among all e.g. LLR, radar and Doppler ranging, optical positional measurements, etc. The capabilities used by PEP to compute the range of observable quantities at some epochs can be summarized as [19]

- to determine the positions and velocities of the centers of mass of the Sun, planets, Pluto, and Earth-Moon barycenter by integrating their equations of motion;
- to solve the equations of motion for the Moon, Moon rotation and Earth (albeit not Earth's rotation);
- to determine the asteroid positions from an elliptic approximation (rather than from integrated equations of motion);
- to calculate the displacement of the lunar reflector with respect to the center of mass of the Moon;
- to calculate the displacement of the ranging station with respect to the center of mass of the Earth;
- to treat photon propagation effects;
- to find a constant bias term for any specified span of data.

PEP calculates all these quantities in the Solar System Barycenter, chosen as the reference frame by the software itself. PEP is able to calculate the O-C residuals of the distances between Observed (O's) and Computed (C's) LLR data, derived from expectations of GR and of terrestrial and lunar Geodesy. These estimates are based on data provided as *normal points*[4] [7]. A normal point (NP) is an alphanumeric string that contains information such as

- date (day, month, year, hour, minute, and second);
- ToF (in 10^{-13} s);
- ToF error (in ps);

[4] In the standard version provided by Nasa JPL.

- array (Apollo 11, Apollo 14, Apollo 15, Luna 1, Luna 2);
- LR station;
- number of photons;
- laser wavelength.

PEP draws a detailed general picture of the solar system over a relatively long time period through ephemerides and initial parameters. The locations of planets and the Moon are contained in the PEP N-body ephemerides, which span the years about 1960 to 2020. The positions are noted at regular intervals, such as 2 days for Mercury, 0.5 days for the Moon, and 4 days for the other planets. O-C (or prefit) refers to the initial stage of processing. PEP can estimate the photon travel time for each launch that it receives in normal point form using the initial parameter values provided, and then compares the result to the real round-trip time that is recorded in the normal point. The theoretically expected range is obtained by means of the encoded physics, which is represented mathematically by the coordinates and partial derivatives contained in the ephemeris at fixed time intervals for each solar system body. During the O-C step, PEP interpolates these partials and determines their values at a given time. Based on its encoded physics, PEP can determine the partial derivatives of the ranges with respect to each of the adjustable parameters, to determine later what adjustments to those parameters will reduce the residuals, producing a better fit. Finally, after completing the O-Cs calculation, PEP proceeds in the formation of normal equations, and parameters estimate. This involves again the basic procedure of least-squares fitting, which requires: an initial set of values of an independent variable, like time; the corresponding measured values of a dependent variable, like round-trip times (ToF) between an observatory and a set of lunar reflectors; a fitting function, which includes some parameters which have to be fit, that represents physics' understanding of the relationship between the two.

7 Conclusions

The work on the MPAc project will continue until the launch date, fixed in April 2024. MPAc must be able to perform two continuous perpendicular rotations to accurately point the frontal face of the CCR towards the Earth. The device is continuously evolving to ensure the success of the mission, which will take place in Ultra High Vacuum space conditions, in a wide operating temperature range. Terrestrial prototypes, with all the characteristics of the final structure, have been developed for the study of mechanical and electronic components. Qualification tests for space are being planned as the components for the Proto Flight Model (PFM) arrived at the LNF. Payload delivery is scheduled for August 2023. MPAc will contribute to attaining lunar orbit range accuracy below a few mm. This will improve, in turn, the precision of the PPN parameters and put more stringent constraints on theoretical gravitational models seen above

with the observations. So, before launching a space mission, it is crucial to conduct a series of tests. One of these also concerns the optical component of the experiment, the CCR. In particular, we attempt to understand what a CCR's light return will be once in orbit by running optical simulations with the Code V software. To get a survey that is as broad as possible and representative of real conditions, we generally investigate several situations. Here, we have shown just the simulations of a perfect uncoated CCR (null DAOs), with a normal incidence of the laser beam (at 532 nm and 1064 nm) and linear polarization. Other optical simulations, which take into account non-zero DAOs, non-normal incidence, circular polarization, and different coatings, are available at the SCF_Lab group. We have been working on improving the code in recent years, and it now allows us to get accurate results that match the theoretical values. Finally, we presented the PEP software. Our future work will first be to improve the code to ensure the accuracy of PEP's results. Furthermore, we would like to modify it to include the equations of motion of the alternative metric theories of gravity. This would be an important step in testing gravitational models beyond GR in the Solar System's context.
The work done so far has been fundamental for the success of the entire project. The MPAc space mission will be a turning point for the LLR measurements.

References

[1] S. Dell'Agnello et al, Nucl. Instrum. Methods Phys. Res. A **692**, 275-279 (2012).

[2] M. Martini et al, Planet. Space Sci. **74**, 276-282 (2012).

[3] NASA Selects Intuitive Machines for New Lunar Science Delivery (2021): https://www.nasa.gov/press- release/nasa-selects-intuitive-machines-for-new- lunar-science-delivery

[4] C. W. Misner, K. S. Thorne, J. A. Wheeler, *Gravitation* (W. H. Freeman and Company, ISBN-10: 0691177791, 1973).

[5] S. Capozziello, A. Troisi, Phys. Rev. D **72**, 044022 (2015).

[6] R. Ruffini, C. Sigismondi, *Nonlinear Gravitodynamics: the Lense-Thirring Effect* (World Scientific Publishing Company, 2003).

[7] L. Mauro, *Reconciling weak and strong field regimes through space missions*, PhD Thesis (2021).

[8] T. W. Murphy, E. G. Adelberger, J. B. R. Battat, C. D. Hoyle, N. H. Johnson, R. J. McMillan, C. W. Stubbs, H. E. Swanson, Class. Quantum Grav. **29**, 184005 (2012).

[9] D. Currie, S. Dell'Agnello, G. Delle Monache, Acta Astron. **68** (7), 667–680 (2011).

[10] L. Rubino, *Testing Gravity with Laser Ranging: LARES-2 and MPAc space missions*, PhD Thesis (2021).

[11] J. G. Williams, L. Porcelli, S. Dell'Agnello, L. Mauro, M. Muccino, D. G. Currie, D. Wellnitz, C. Wu, D. H. Boggs, N. H. Johnson, accept. Planet. Sci. J. AAS IOP, (2023).

[12] E. Ciocci, M. Martini, S. Contessa, L. Porcelli, M. Mastrofini, D. Currie, G. Della Monache, S. Dell'Agnello, Adv. Sp. Res. **60**(6), 1300-1306 (2017).

[13] J. J. Degnan, *A tutorial on retroreflectors and arrays for SLR*, ILRS Workshop, Frascati, Italy (2012).

[14] T. W. Murphy Jr., S. D. Goodrow, Appl. Opt. **52**, 117-126 (2013).

[15] J. B. R. Battat, C. W. Stubbs, J. F. Chandler, Phys. Rev. D **78**, 022003 (2008).

[16] R. D. Reasenberg et al., Astrophys. J. Lett. **234**, L219 (1979).

[17] J. F. Chandler, R. D. Reasenberg, I. I. Shapiro, *Proceedings of the 7th Marcel Grossman Meeting on recent developments in theoretical and experimental general relativity, gravitation, and relativistic field theories* (edited by Jantzen R. T., Mac Keiser G., Ruffini R., 1996).

[18] I. Shapiro, R. D. Reasenberg, J. F. Chandler, Phys. Rev. Lett. **61**, 2643-2646 (1988).

[19] N. H. Johnson, *High-Precision Lunar Ranging and Gravitational Parameter Estimation With the Apache Point Observatory Lunar Laser ranging Operation*, University of California San Diego (2015).